

Paper presented at the Int. Lightning Detection Conference, Tucson, Nov. 1996

Detection Efficiency and Site Errors of Lightning Location Systems

Schulz W. Diendorfer G.

Austrian Lightning Detection and Information System (ALDIS)

Kahlenberger Str. 2b

1190 Vienna, Austria

Abstract

Detection efficiency (DE) is one of the most important system performance parameters of a lightning location system. We present a theoretical model for the DE, which does not need the assumption of a theoretical peak current distribution. For testing the model we split the Austrian lightning location network into two separate networks. After correcting the number of flashes of the two different networks for DE we get about the same value for both networks.

In the second part of this paper we show, that the cable connections of the direction finder have a significant influence on the site error of a sensor.

1. Detection Efficiency

The most important performance parameters of lightning location systems are the so-called detection efficiency (DE) and the location accuracy. Although the DE is a very important parameter, quite often insufficient attention is paid to the DE in literature dealing with data from lightning location systems. In many papers important system parameters (e.g. threshold values of the sensors and network configuration), which strongly affect the DE, are not reported. Most of the published lightning current distributions or lightning density plots based on lightning location data are presented without any comments on the DE. To be able to compare lightning peak current distributions for different regions or even for the same region determined by different location systems the detection efficiency has to be involved. Otherwise there is a high risk to draw a wrong conclusion.

Determination of ground truth data (the real number of flashes or strokes occurring at a certain location) requires a high experimental effort (video cameras) [Mach et al., 1986] and therefore theoretical models are normally used to estimate the detection efficiency of a location system. In this paper we present a model to estimate the network DE for a certain current peak amplitude. This model allows to correct lightning peak current distributions or ground flash densities based on lightning location data. The corrected current distribution or ground flash density should be as close as possible to the ground truth data.

If we talk about DE of a location system, it is necessary to distinguish between two different types of DE, the stroke detection efficiency and the flash detection efficiency [Rubinstein, 1995]. The flash detection efficiency is defined as the fraction of flashes detected from the total number of flashes occurring in reality. The stroke detection efficiency is defined the same way regarding the individual strokes. Rubinstein [1995] has shown, that the relation between stroke and flash DE strongly depends on the distribution of the number of strokes per flash and that the flash DE can be significantly higher

than the stroke DE.

To be able to locate a lightning flash with a MDF system a minimum of two sensors reporting the flash is required.

1.1 Detection efficiency model

The model presented in this contribution is applied to calculate the flash DE and therefore the DE mentioned in the following chapters always means the flash DE. To be able to estimate the detection efficiency for a certain region covered by a given location network and for a specified lightning peak current it is necessary to assume a sensor detection efficiency function. For a specified peak current this function of DE versus distance D is basically defined by three parameters

- 1) the maximum sensor detection efficiency,
- 2) the saturation limit and
- 3) the threshold limit.

Fig. 1 shows an idealized sensor DE function, where the distances D_1 and D_2 are related to the DF saturation and threshold limits respectively. Both values depend on the lightning peak current, on the angle of incidence and on the waveform distortion due to finite ground conductivity. The sensor DE function in Fig. 1 is idealized, because in reality no sensor detects 100% of all of the flashes within the limits of saturation and threshold. Local noise, dead times, waveform discrimination etc. will always cause a certain limitation of the DE to less than 100% even in the range of normal system operation.

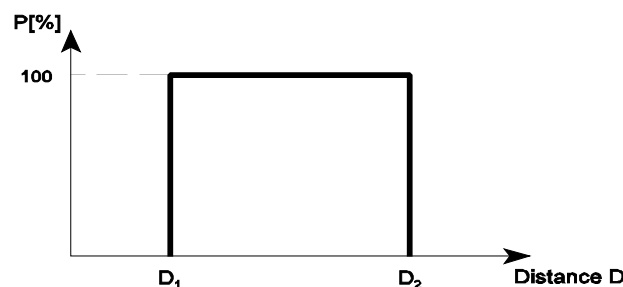


Fig. 1: Idealized sensor DE for a specified peak current and angle (D_1 ... saturation limit, D_2 ... threshold limit)

The distance limits D_1 and D_2 are calculated with the aid of the transmission line model and an exponential attenuation factor b [Orville, 1991; Idone et al., 1993]. The attenuation of the electromagnetic field is caused by the propagation over ground of finite conductivity. If a flash of the specified peak current occurs at a distance $D < D_1$, the sensor will be saturated. If the striking point is at a distance $D > D_2$, the signal at the sensor site will not exceed the threshold limit and therefore not trigger the sensor. A first step in the assumption of a more realistic sensor DE is to reduce the maximum sensor DE to less than 100% (see Fig. 2). This reduction accounts for the missing of a certain percentage of flashes, e.g. when the flash occurs during the dead time of the sensor. If the sensor processes a flash, it has a dead time of 4 ms. During that time the DF does not accept a further signal.

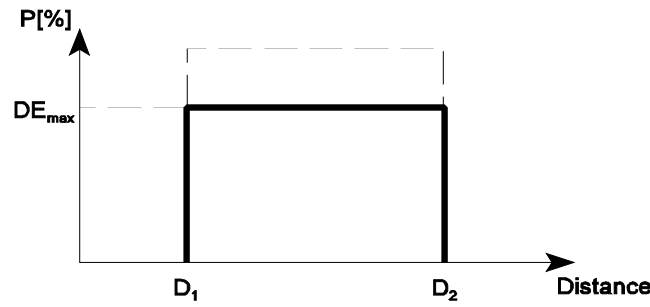


Fig. 2: Sensor DE function with $DE_{max} < 100\%$

A direction finder (ALDF) is triggered, if the absolute signal of one of the two magnetic antennas crosses the enable threshold. Therefore the sensor DE varies with the angle of incidence. To trigger the sensor, signals with an angle of incidence of 45° have to be about 40% higher than signals in direction of one of the antenna axis. The DF is already saturated, if only one of the signals of the two antennas is larger than the saturation limit. Therefore, also the saturation limit depends on the angle. This model takes into account the dependency of saturation and threshold limit from the angle of the field incidence as described above.

A field signal just crossing the trigger level will usually not satisfy the waveform criterias. Therefore we define the trigger level for our DE analysis as the level, where the field is at least twice as high as the adjusted threshold level.

A further improvement to make the sensor DE more realistic is an adaption of the instant change of the DE at the saturation and the threshold distance. It is very unlikely, that the sensor does not detect any flashes, if they are closer than the calculated saturation distance D_1 or more distant than the threshold distance D_2 . Instead of an instant change we assume a more continuous increase and decrease of DE at the saturation limit and the threshold limit respectively (Fig. 3).

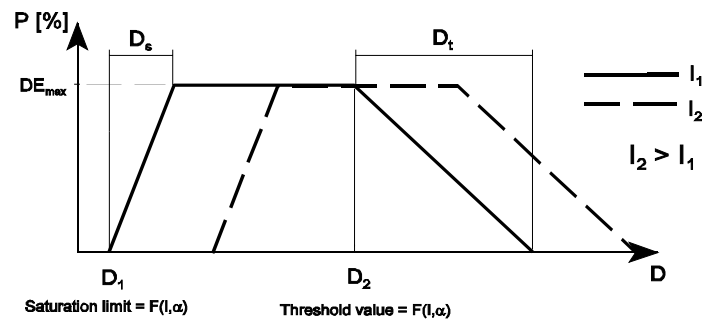


Fig. 3: Sensor detection efficiency for two different peak currents I_1 and I_2 (D_s ... saturation range, D_t ... trigger range)

Several analysis have shown, that the slope at the saturation limit does not affect the result of the detection efficiency very much. The slope is high compared to the slope at the threshold limit. The saturation limit is a quite sharp limit. A more continuous decrease of DE was observed at the threshold limit. Fig. 3 shows a schematic function of the detection efficiency for two different peak currents I_1 and I_2 . It is obvious that I_1 is smaller than I_2 , because I_2 saturates the DF at longer distances D_1 . On the other hand peak current I_2 triggers the sensor up to a longer distance D_2 .

A very important parameter of this DE model is the exponential attenuation factor b according to Orville [1991] or Idone et al. [1993]. The transmission line model predicts a signal strength proportional to D^{-1} , but does not take into account the ground conductivity. To account for the ground conductivity it is necessary to calculate the peak field attenuation over distance not with D^{-1} but with D^{-b} where $b > 1$. To estimate the damping factor b , the individual DF signal amplitudes versus distance are plotted and a power curve of the form $y = ax^b$ is fitted, where y is the amplitude and x is the distance from the optimized flash location. Fig. 4 shows an example of this approximation with data from the Austrian lightning detection system.

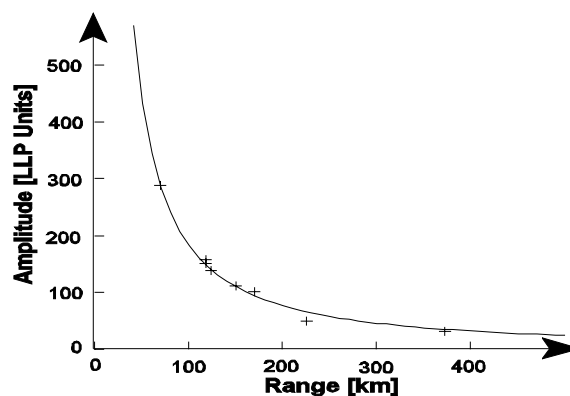


Fig. 4: Power fit to signal strength data from 8 DF ($b = -1.27$)

The attenuation factor b depends on the ground conductivity of the individual regions of the network. To get a mean attenuation factor valid for the entire network, a set of almost regular distributed strokes detected by at least 6 DF was extracted from the lightning database. With this 2885 strokes a mean attenuation factor of $b = -1.23$ was calculated. Contrary to Orville [1991] and Idone et al. [1993] the attenuation factors of this investigation were calculated by a nonlinear least square fit because this gives the most probable parameter b . Orville and Idone used a linear least square fit to transformed data.

The other unknown values of the sensor DE function were estimated by investigating the relative sensor DE of the sensor number 4 in Niederöblarn, which is the central sensor of the Austrian network. Fig. 5 shows the percentage of flashes located by DF 4 from the total number of flashes located by the entire network for different peak currents. For each peak current the area under investigation around the DF was adjusted to the trigger distance D_1 for the assumed peak current. Not only flashes with the exact

peak current were extracted but also flashes with amplitudes of ± 2.5 kA.

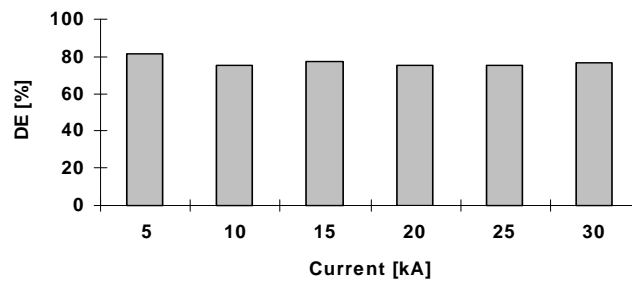


Fig. 5: Sensor DE for different current amplitudes

A relative sensor DE in the range from 75% to 80% becomes obvious from Fig. 5. Because it is still unknown, how many flashes are not detected by the system at all, the absolute sensor DE is assumed to be about 10% smaller than the relative sensor DE. A reduction by 10% seems to be an acceptable number for this region of the network.

To estimate the ranges D_s and D_t , data from our location system were analyzed to determine the change of the relative sensor DE with distance. Because the sensor DE depends on the angle and the peak current, it was necessary to perform this investigation for different angles and peak currents. As an example Fig. 6 shows the results for DF 4 for an angle of $135^\circ (\pm 10^\circ)$ and an amplitude of 20 kA (± 2.5 kA). The threshold distance $D_2=160$ km is calculated with the transmission line model and a damping constant $b=-1.23$, for an amplitude of 20 kA, an angle of 135° and a threshold value of 70mV.

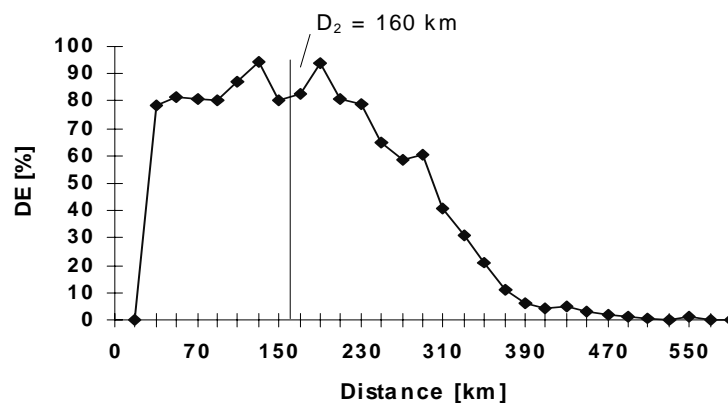


Fig. 6: Dependency of sensor DE on the distance for peak currents 20 kA, angle 135° and threshold 70mV

Fig. 6 shows for small distances a rapid increase of sensor DE to about 80% and for a distance of about 410 km the sensor a DE of almost zero. From similar investigations for different peak currents and directions we estimated the distance D_s , which does not influence the result significantly, to about 20 km and the distance D_t to 250 km. Fig. 6 also shows, that the calculated threshold distance D_2 is reasonable.

Up to now, only the detection efficiency function for a specified peak current and angle to the flash location of the individual sensor is defined. The flash peak current in this model is defined as the highest peak current of all of the strokes of a flash. The efficiency for a two DF network to detect a specified peak current I_p is calculated by

$$DE = p_1 * p_2 \quad (1)$$

where p_1 and p_2 are the probabilities of sensor 1 and sensor 2 to register the flash (dependent on the distance to the flash) of a certain peak current respectively. This is called the **peak current network DE**. For a three DF network the DE is calculated by

$$DE = p_1 * p_2 * q_3 + p_1 * q_2 * p_3 + q_1 * p_2 * p_3 + p_1 * p_2 * p_3 \quad (2)$$

where p_i is the probability, that the flash is detected by the i -th DF and q_i is the probability for the i -th DF to miss the flash ($p_i=1-q_i$). Contrary to the probability approaches from e.g. Tuomi [1990] or Rubinstein [1994] this model takes into account the threshold values and the modification of amplitude and waveshape. Therefore the DE should not be overestimated with this model as done by some other models [Sorenson, 1995].

Now we can calculate the probability for detecting a lightning with specified peak current and with the given network (**peak current network DE**). Lightning peak currents are statistically distributed and therefore we have to calculate the peak current network DE for different amplitudes. Two different approaches to calculate the **total network DE** in a certain region are possible:

Method 1: Calculation of the detected lightning distribution in a certain area from an assumed theoretical distribution (e.g. Berger distribution) representing 100% of cloud to ground flashes. The ratio of the two distributions is the estimated **total network DE** in this area.

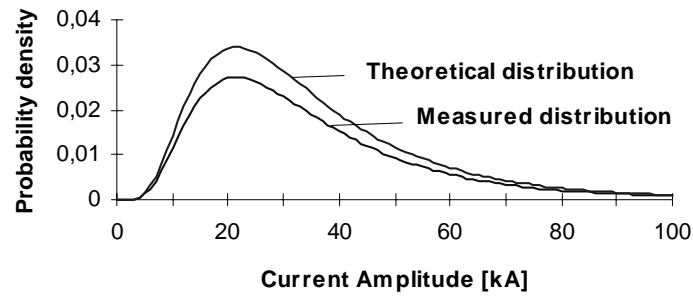


Fig. 7: Correction from a theoretical distribution

Method 2: Correction of the detected peak current distribution in a region (e.g. 10km x 10km) to a “natural” lightning current distribution. The frequency of each current amplitude is corrected by the corresponding **peak current network DE** (Fig. 8). The **total network DE** regarding the total distribution of peak currents is given by the ratio of the sum of detected frequencies to the sum of corrected frequencies.

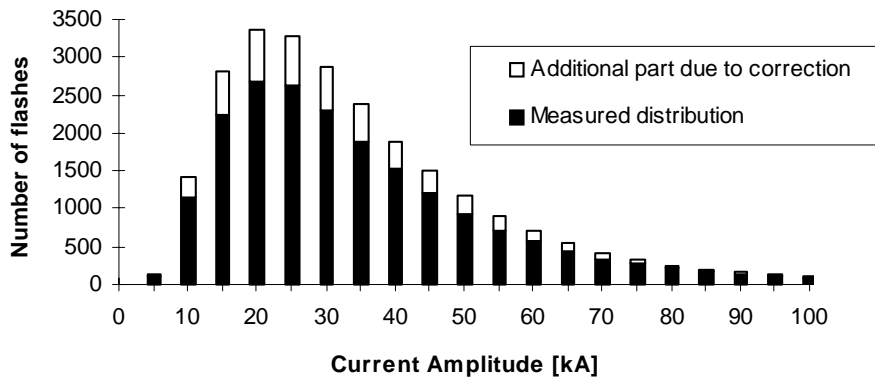


Fig. 8: “Natural” peak current distribution as the sum of detected flashes plus missed flashes due to the limited DE

It is very important to note that for this approach of calculating the **total network DE** it is not necessary to assume a certain natural peak current distribution as required for the previous method.

To get DE information for the entire network the **total network DE** has to be calculated for uniformly distributed areas over the network (e.g. 10x10 km² segments). From this data it is possible to produce DE contour plots. This process applies for both methods.

1.2. DE calculation from a measured distribution by applying method 2

Because the assumption of a peak current distribution has a high influence to the result of the calculated DE, we prefer using method 2 for the DE calculation. For testing the DE model and all the derived parameters, we compare results for an assumed 3 DF network and the 8 DF network in Austria. If the model is sufficient, the corrected ground truth flash number should be the same for both networks. Flashes only seen by the assumed 3 DF network (see Fig. 9) DF 1 (Eggelsberg), DF 6 (Fürstenfeld) and DF 8 (Dobersberg) were extracted from the database.

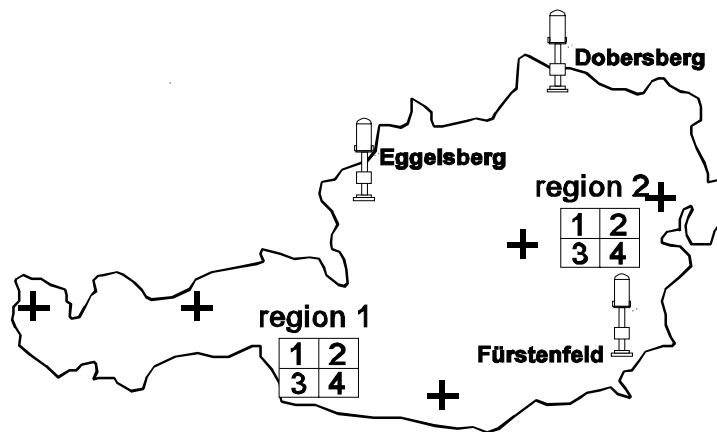


Fig. 9: 3 DF network with 2 different regions of investigation

Two regions were investigated. Each region was split into four different rectangles and inside these rectangles all the flashes seen by the 3 DF network and the 8 DF network were counted. With the previously described model we have calculated the DE for all the rectangles from the measured peak current lightning distribution of the Austrian lightning detection network in 1994. We assumed a damping factor $b=-1.23$, a maximum sensor DE of 70%, a saturation range of 20 km and a threshold range of 250 km. The threshold value in the Austrian system is set to 70 mV and this value was also used for our calculations

Table 1: 3 DF network (region 1)

rectangle	detected flashes	calculated DE [%]	estimated number of ground truth flashes
1	589	31	1900
2	545	45	1211
3	515	24	2141
4	653	37	1765

Table 2: 8 DF network (region 1)

rectangle	detected flashes	calculated DE [%]	estimated number of ground truth flashes
1	1984	97	2045
2	1479	98	1509
3	1898	95	1998
4	1576	96	1641

Table 3: Deviation of ground truth data related to the 8 DF network in % (region 1)

rectangle	deviation [%]
1	+7
2	+20
3	-7
4	-7

Table 4: 3 DF network (region 2)

rectangle	detected flashes	calculated DE [%]	estimated number of ground truth flashes
1	225	72	313
2	825	70	1179
3	791	70	1130
4	800	68	1176

Table 5: 8 DF network (region 2)

rectangle	detected flashes	calculated DE [%]	estimated number of ground truth flashes
1	318	98	324
2	1052	97	1085
3	1183	98	1207
4	1208	97	1245

Table 6: Deviation of ground truth data related to the 8 DF network in % (region 2)

rectangle	deviation [%]
1	+3
2	-9
3	+6
4	+6

Although the absolute numbers of flashes for the 3 DF network and the 8 DF network are different by

more than 300 % (region 1) the mean absolute deviation after the correction in both regions is about 8%. This is in the range of the expected accuracy of the model and therefore Tables 1 to 6 clearly show that the model can be used to calculate sufficiently the network DE. Fig. 10 shows a DE plot for the Austrian network with the same parameters as used in the previous analysis.

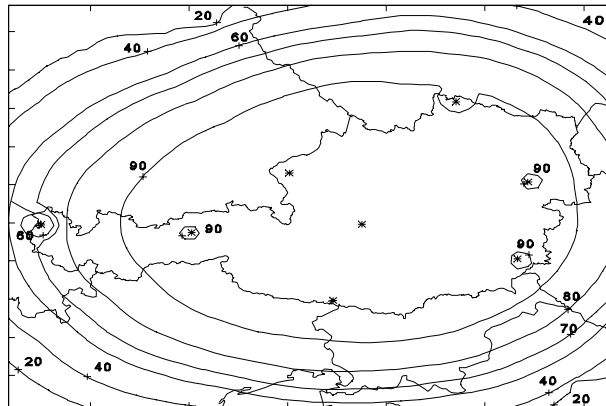


Fig. 10: DE of the Austrian network with threshold 70 mV

2. Change of site error for DF 8 in Austria

In spring 1996 it was necessary to move DF 8 (Dobersberg) of the Austrian network by about 20 m in direction NNE. This DF is located at a small airport in the northern part of Austria (see Fig. 9). Fig. 11 shows a map of the site with the new and the old location of this DF.

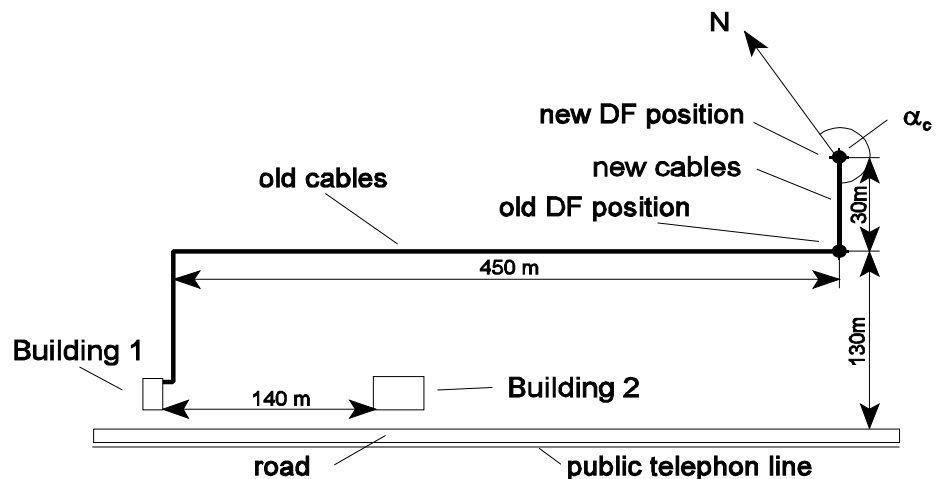


Fig. 11: Map of the site of DF 8

The DF is connected by two shielded cables to the telephone line and the local power supply. Fig.12 shows the original grounding conditions for the power cable, where the cable shield was connected to ground at both ends.

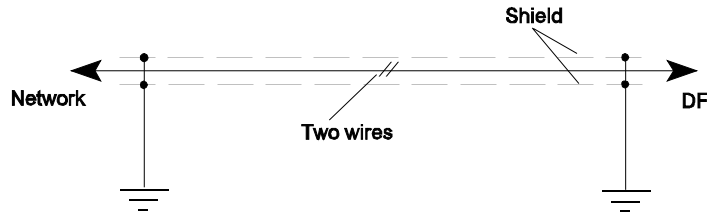


Fig. 12: Grounding conditions of the power cable

After the replacement of the DF the old cables were extended by new cables as shown in Fig. 11. The type of all the used cables is given in Table 7.

Table 7: Types of cables

	old cable	new cable
power supply	2 x 1.5 mm ² + shield wire	5 x 2.5 mm ² +shield wire
communication	8 x 0.75 mm ² + shield wire	8 x 0.75 mm ² +shield wire

The shield wires of the cables were originally connected to ground at both ends. Earthing at the DF site is achieved by an earth wire (about 10m length) buried in the same direction as the cables.

It is important to note that there is no obstacle around the DF in a radius of about 300m except the telephone line (see Fig. 11). With these quite good site conditions a site error of an amplitude of less than three degree was expected.

A site error analysis was done before and after the movement of the DF and showed significant differences. At the old location of the DF the amplitude of the site error was about five degrees (see Fig. 13), although the site conditions were quite good as mentioned before.

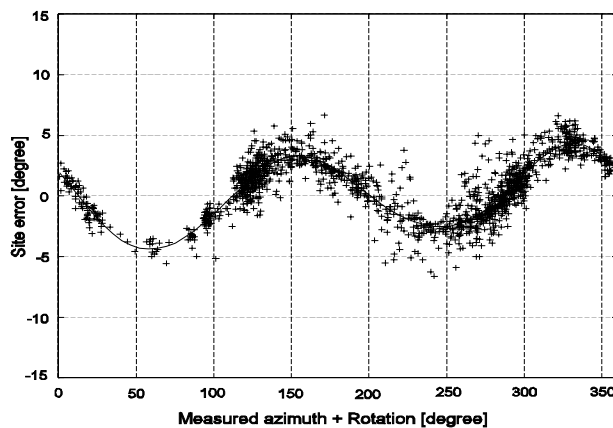


Fig. 13: Original site error of DF 8

The original site error is almost a two cycle sinusoidal function as predicted by the theory.

The site error investigation after moving the DF revealed a misalignment (rotation) of the DF by about 8° and an increase of the maximum error to about 13° .

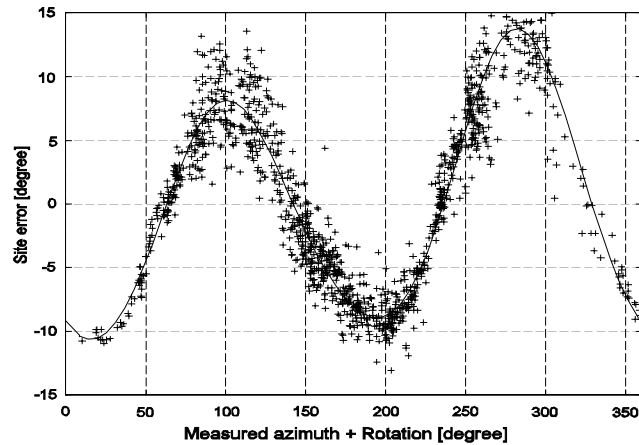


Fig. 14: Site error of DF 8 after moving the DF

A comparison of Fig. 13 and Fig. 14 shows that the amplitude has increased significantly and that the phase of the error function has shifted by about -90° .

Because the direction of the cable (α_c) has changed by about -90° (see Fig. 11) in the new installation, a shift of -90° in the new site error function suggested that the cable itself has an important influence on the site error. A further investigation showed that almost exactly in the direction of the cable $\alpha_c = 220^\circ$ (see Fig. 11) the site error function crosses the zero degree line with a positive gradient. With this information the site error functions of the other Austrian DF were investigated more detailed. As a result of this investigation we found that all the DF with well defined site error functions show a zero crossing with positive gradient in the direction of the cable. This could be explained in the following way:

In Fig. 15 a lightning stroke with a lightning current flowing down to ground and a cable in a direction of $\alpha_c = 180^\circ$ is assumed.

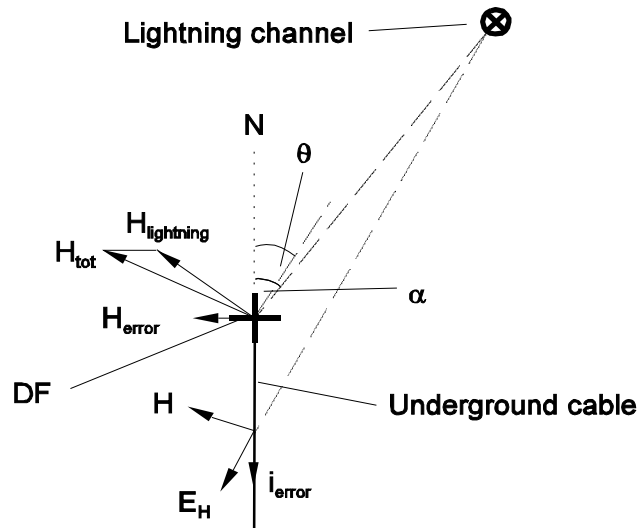


Fig. 15: Site error of an underground cable

If infinite ground conductivity is assumed, no horizontal electric field at ground level exists at far distances from the lightning stroke. Due to finite ground conductivity a component of the pointing vector points in direction to the ground and thus in the example above the horizontal electric field points in the direction shown in Fig. 15. The component of the horizontal field parallel to the cable causes a current i_{error} in the cable (shield and wires), which is always flowing in cable direction (north-south direction). The magnetic field of this current is perpendicular to the induced current i_{error} in the cable. Independent of the location of the lightning discharge, the re-radiated field due to the current i_{error} is always in the east-west direction. Thus an additional magnetic field H_{error} will be measured by the north-south DF loop, causing the DF to measure an erroneous magnitude of the east-west field. The direction of the error field H_{error} is drawn under the assumption that the antenna is above ground and thus above the cable. In case of a lightning stroke in the first quadrant of the DF, the angle difference $\alpha - \theta$ is greater than zero. The sign of the angle difference is independent of the lightning current polarity (pos. or neg. stroke). In the second quadrant of the DF the angle difference $\alpha - \theta$ is less than zero. In total this effect results in the well known two cycle sinusoidal function.

This basic arrangement also predicts a zero crossing of the site error function in the direction of the cable.

Further it was investigated, how the site error is affected by the connection of the shielding wires of the power and the communication cable to the earthing system. This was done in three steps:

1) Ground connection of the power cable shield was opened at building 1 (see Fig. 11), the communication cable remains unchanged.

- 2) Opening of the connection to ground of the power cable shield at the DF end, communication cable shield still connected to ground at both ends.
- 3) Opening of the connection to ground of the communication cable shield at both ends (both cable shields floating).

After each change of the grounding conditions at the cable ends a new site error analysis was performed. Fig. 16 shows the calculated site error functions for the four different grounding conditions.

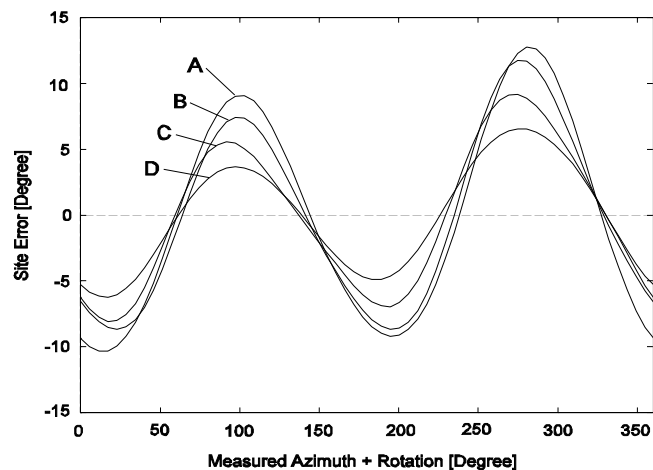


Fig. 16: Site error functions for different grounding conditions of the cable shields
 A) Original site error after the DF movement (cable shields grounded at both ends).
 B) Shield wire of the power cable only grounded at the DF end
 C) Power cable floating
 D) Both cables floating

Fig. 16 reveals a 50 % reduction of the original site error and therefore justifies our assumption of a significant influence of the cable shield connections on the site error function. It is important to note that also the rotation RO decreased by about 50%.

3. Discussion

In the first part of this contribution we presented a new detection efficiency model and the related calibration. With this model it is possible to calculate the **total network DE** without the assumption of a lightning peak current distribution. For the test of the model, the measured lightning location system peak current distribution of the year 1994 is used for the entire region of the network assuming that this distribution is valid for the whole region. If this is not true, we could also extract a lightning peak current distribution for each region for the calculation of the DE in this region. But this approach requires a lot of data in each individual region, because an almost complete lightning peak current distribution is necessary for the correction. It is not possible to correct the number of flashes for a certain amplitude, if there are no flashes detected with this amplitude.

In the second part we have shown that the cables to the direction finder have a significant influence to the site error function. The appearance of a significant rotation after movement of the DF suggests that the change of the direction of the cable has a major influence on the rotation.

It would be interesting to test, if the site errors were further reduced in case of a DF not connected by conducting cables at all (e.g. battery power supply and fiber optic data transmission). On the other hand it is questionable, if it makes sense to reduce the site error in this way, because there are methods available for the site error correction.

References:

MACH D.M., D.R. Mac Gorman, W.D. Rust, R.T. Arnold: Site errors and detection efficiency in a magnetic direction finder network for locating lightning strikes to ground, J. of Atmospheric and Oceanic Technology, Vol. 3, 67-74, 1986.

ORVILLE R.E.: Calibration of a magnetic direction finder network using measured triggered lightning return stroke peak currents. J. Geophys. Res., Vol. 96, 17135-17142, 1991.

IDONE V.P., A.B. Saljoughy, R.W. Henderson, P.K. Moore, R.B. Pyle: A reexamination of the peak current calibration of the national lightning detection network.

RUBINSTEIN M.: On the estimation of the stroke detection efficiency by comparison of adjacent lightning location systems. ICLP 1994.

RUBINSTEIN M.: On the determination of the flash detection efficiency of lightning location systems given their stroke detection efficiency. EMC conference, Zürich, 1995

SOERENSEN T.: Lightning registration systems analysis, optimization and utilization. Ph.D. Thesis, Electric Power Engineering Department, Technical University of Denmark, 1995.

TUOMI T.: On the accuracy and detection efficiency of a lightning location system of four direction finders. Geophysica (1990) 26, 2, pp. 1-16. Finnish Geophysical Society, Finland, 1990.